Short Note

On the simulation of nearly inviscid two-dimensional turbulence

D.G. Dritschel *, R.K. Scott

School of Mathematics and Statistics, University of St Andrews, St Andrews, North Haugh, KY16 9SS Scotland, United Kingdom

We here compare two numerical algorithms in a simple test case involving the simulation of two-dimensional freely-decaying turbulence. The first is a standard pseudo-spectral algorithm, as has been widely used in studies of this problem. The second is a less well known hybrid Eulerian–Lagrangian algorithm based on contour dynamics. The comparison verifies the near equivalence, in detail, of the two algorithms at early times. At later times, significant advantages of the second algorithm become clear, in particular the ability to achieve a much higher effective Reynolds number at a negligible fraction of the computational effort. Specifically, a comparable simulation using the pseudo-spectral algorithm would take $\mathcal{O}(10^8)$ times more computer power.

We solve the two-dimensional Navier–Stokes equation in vorticity form

$$\omega_t + J(\psi, \omega) = \nu\nabla^2\omega; \quad \omega = \nabla^2\psi \tag{1}$$

in a doubly-periodic domain and using a simple random initial condition, as specified below. Here ω is the vorticity, ψ is the streamfunction, J is the Jacobean and ν is the viscosity coefficient.

The initial conditions for (1) are constructed by specifying an initial energy spectrum of the form $E(k) = ak^8\exp[-8\pi(k/8)^2]$, where $k = |\mathbf{k}|$ is the wavenumber, with random phases for all Fourier coefficients. This $E(k)$ is peaked at $k = \sqrt{32/\pi} \approx 3.2$ and is more than 10^{36} times smaller by $k = 32$. The coefficient a is chosen to give unit r.m.s. velocity, or energy per unit area $\frac{1}{2}\langle|\nabla\psi|^2\rangle = \frac{1}{2}$. The maximum initial velocity is about 2.3, while the peak vorticity $|\omega|_{max} = 11.942$ and the (initial) r.m.s. vorticity $\omega_{rms} = 3.541$.

First, we solve (1) using a standard pseudo-spectral algorithm and a fourth-order Runga–Kutta time scheme. Approximate de-aliasing is achieved using a spectral filter following [6], with parameters as specified in [5], hereafter DTS. The viscous term is treated exactly by means of an integrating factor. We perform a series of integrations at resolutions $N = 512$, $1024, 2048, 4096$, and 8192, where N is the number of grid points in x and y. In each case the time step is chosen to be $0.0025(512/N)$. This time step is less than half the CFL time step required for stability at the initial time and is verified *a posteriori* to never exceed 75% of the CFL time step during the flow evolution. In tests using resolutions up to $N = 2048$, halv-

---

* Corresponding author. Tel.: +44 1334 463721; fax: +44 1334 463748
  E-mail address: dgd@mcs.st-and.ac.uk (D.G. Dritschel).

ing the time step had no measurable impact on solution accuracy. A viscosity coefficient $v = 4\pi/(3N/8)^2$ is chosen based on the initial vorticity to ensure adequate dissipation of enstrophy $Q \equiv \frac{1}{2}\langle\omega^2\rangle$ at high wavenumbers.

Second, we perform a single integration of (1) with $v = 0$ using the Contour–Advective Semi-Lagrangian (CASL) algorithm [3]. The CASL algorithm does not use any explicit viscosity, but removes vorticity filaments below the grid scale by a method called "contour surgery" [2]. The algorithm represents the vorticity field by a set of contours across which the vorticity jumps discontinuously by a fixed amount $\Delta\omega$, which can be chosen according to the desired level of accuracy. The algorithm represents the velocity field on a conventional periodic grid and this velocity is interpolated to the contour nodes using a standard bi-linear interpolation. The contours are advected using a fourth-order Runga–Kutta time scheme. The velocity field is obtained from the contours by a fast-filling routine and inversion of $\omega = \nabla^2\psi$ in spectral space. We have used the following standard numerical parameters in the integration reported: a basic grid size of 512×512 (used for carrying out the inversion and representing the gridded velocity field), a grid 4 times finer in each direction for fast-filling, 80 contour levels with vorticity jump $\Delta\omega = 0.251328$ spanning the entire range of ω, a surgical scale $\delta = \pi/5120$ equal to a twentieth of the inversion grid scale, a large-scale length $L = 1$ and a dimensionless node separation parameter $\mu = 2\sqrt{\delta/L} = 0.0495416$ for representing the contours, and a time step $\Delta t = 0.025$. We have performed two additional integrations using values of $\Delta\omega$ half and double of this value and have verified that the results obtained are insensitive to this choice.

The pseudo-spectral integrations are described fully in DTS; here we focus on the comparison between the two numerical methods. Both qualitative (visual) and quantitative comparisons are made. Fig. 1 shows the vorticity field ω in the full domain at $t = 5$ (top) and at $t = 9$ (bottom) for the 8192^2 pseudo-spectral integration (left) and the CASL integration (right). At both these times, the fields match closely. The agreement is astonishingly close at $t = 5$, despite the highly nonlinear dynamics and the complex vorticity structures that have developed by this time. Indeed at $t = 5$ it is difficult to detect *any* differences in the two vorticity fields at the level of these plots.

The level of agreement is demonstrated further by a zoom into 1/64th of the domain shown in Fig. 2 (top row for $t = 5$ and bottom row for $t = 9$). Again at $t = 5$ the two integrations can be seen to agree extremely well down to the smallest-scale structures of the flow. Differences can be seen, for example in the downward turning lip to the left of the central dark oval, which is slightly more diffuse in the pseudo-spectral integration, a direct effect of viscosity. In the CASL integration on the other hand, this structure has evolved inviscidly, since the scales involved are still well above the surgical scale δ. It is worth
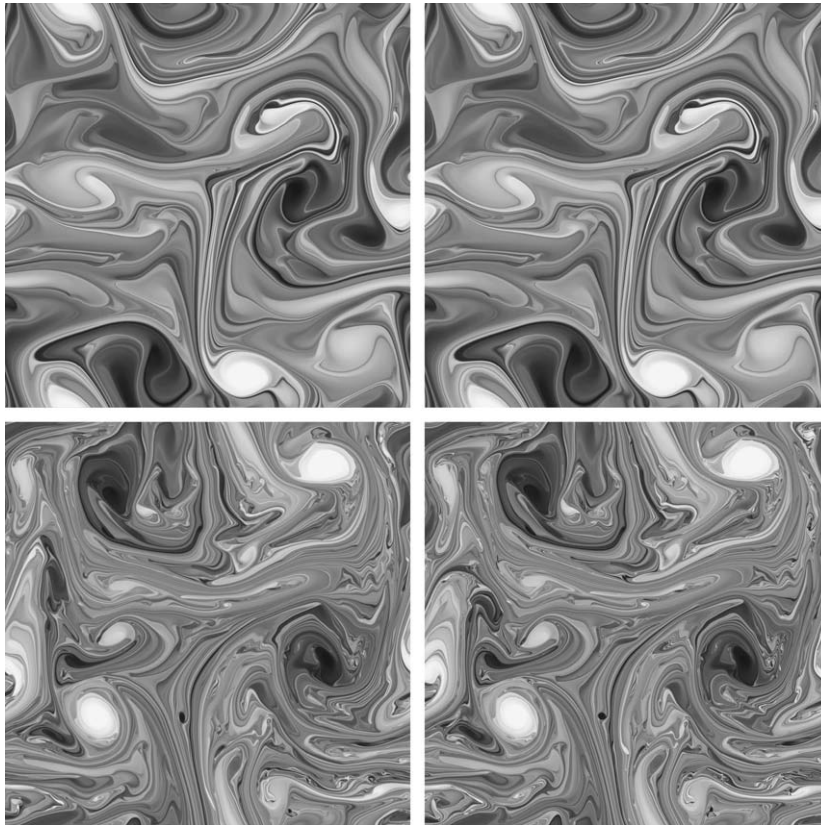
Fig. 1. Full domain comparison of the vorticity field in the 8192^2 pseudo-spectral integration (left panels) and in the CASL integration (right panels) at time $t = 5$ (upper panels) and at $t = 9$ (lower panels). A linear grey scale is used between $-10 < \omega < 10$ (black being most negative) and values with $|\omega| > 10$ are saturated to improve contrast.
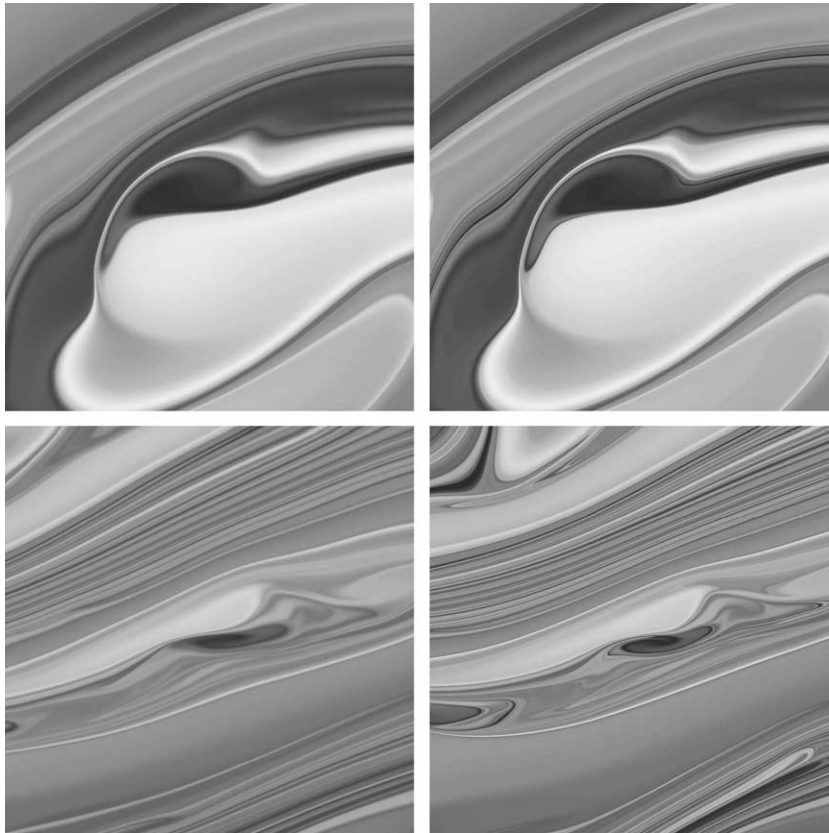
Fig. 2. Magnification of 1/64th of the domain shown in Fig. 1.

noting that this close agreement is achieved despite the relatively coarse discretisation of vorticity levels in the CASL algorithm (80 levels across the full vorticity range). The discrete levels are just visible in Fig. 2 (top right), particularly in the larger regions of weak vorticity gradient. More levels can be used at a modest additional cost proportional to the extra number of contour nodes required [3,4].

Time $t = 9$ corresponds to the time of peak complexity, or, equivalently, the time of maximum enstrophy dissipation $-\frac{1}{2}d\langle\omega^2\rangle/dt = -\dot{Q}$, for the 8192^2 pseudo-spectral integration. The complexity of the vorticity field increases until this time due to repeated stretching and folding by the turbulent flow and then decreases as the (cumulative) enstrophy dissipation increases (see DTS for full details and also Fig. 5 below). The complexity is clear in both the full fields and in the magnifications (lower panels in Figs. 1 and 2). At this later time there is also close agreement in the general features of the two integrations, but now there are also significant differences.
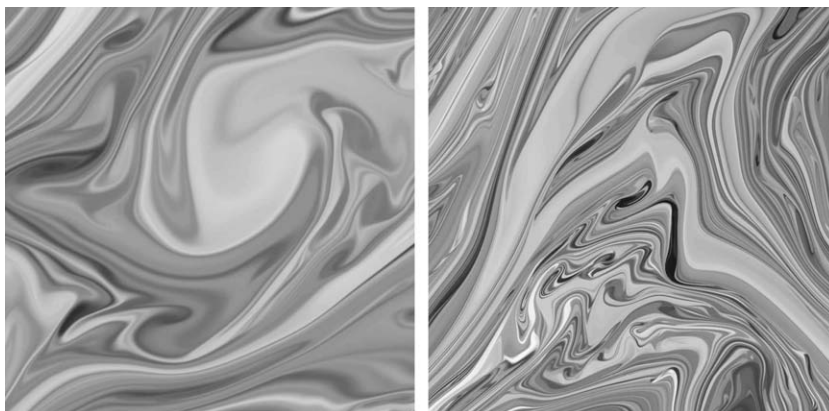
Fig. 3. Magnification of 1/64th of the domain at $t = 15$, from the 8192^2 pseudo-spectral integration (left) and from the CASL integration (right).
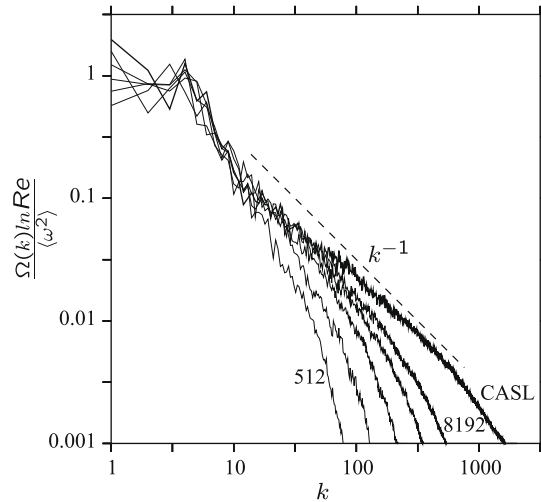
Fig. 4. The scaled enstrophy spectrum $\Omega(k, t) \ln Re / \langle \omega^2 \rangle$ at the time of peak enstrophy dissipation and for all of the integrations performed. The CASL results are in bold.

One inevitable difference arises from the extreme nonlinear and chaotic nature of the flow, which will always lead to divergence of the two solutions with time. Differences associated with such nonlinearity are typically seen as differences in the position or shape of larger-scale structures, such as the coherent light region on the extreme left hand edge in Fig. 1, or the upper left corner of Fig. 2 (lower panels). This is an inherent limitation imposed by the characteristic behaviour of turbulent flow.

A second difference arises from the viscous dissipation in the pseudo-spectral integration. This can be seen most clearly in the highly filamentary regions of Fig. 2. Although the pseudo-spectral integration is capable of capturing an impressive degree of filamentation at this resolution, it is nevertheless visibly more diffuse than the CASL integration. In the former case, filament amplitudes at the smallest scales are strongly reduced by viscosity. By contrast, in the latter case, provided a filament keeps a transverse scale larger than the surgical scale δ, it will remain completely unaffected by surgery.

In the CASL integration, the peak enstrophy dissipation $-\dot{Q}$ occurs just after $t = 15$, somewhat later than in the 8192^2 pseudo-spectral integration. At this time, the vorticity field has attained a degree of complexity on which surgery becomes significant. By this time the pseudo-spectral integration at 8192^2 is in a period of strong decay. The vorticity fields for each case at $t = 15$ are shown in Fig. 3, again with a magnification showing 1/64th of the domain. Most of the structure present in the pseudo-spectral integration at $t = 9$ has been dissipated, while that in the CASL integration has increased further in complexity.
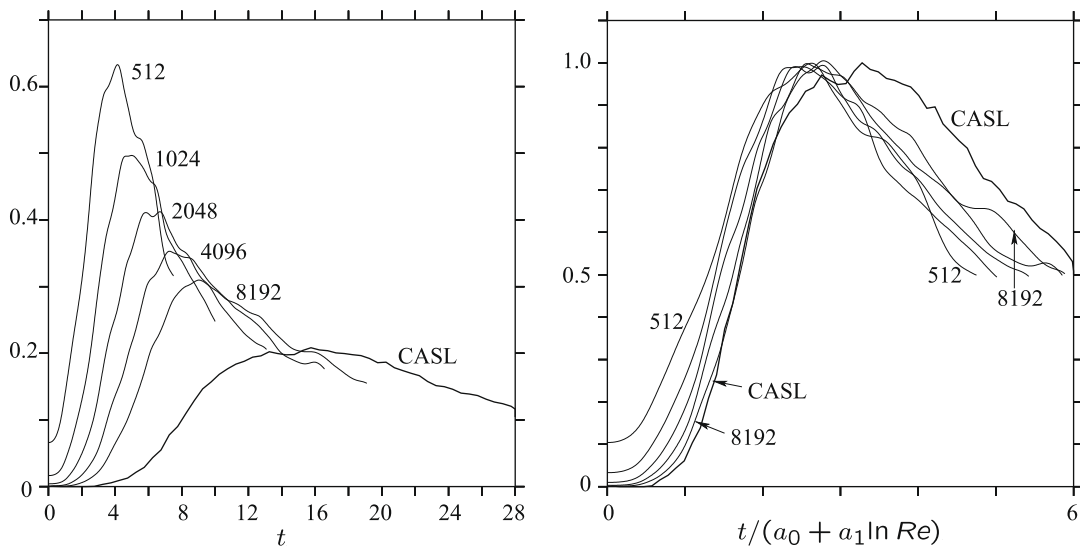
Fig. 5. Enstrophy dissipation $-\dot{Q}$ versus time t (left) and scaled enstrophy dissipation $-\dot{Q}(a_0 + a_1 \ln Re)$ versus scaled time $t/(a_0 + a_1 \ln Re)$ (right), for all of the integrations performed. The CASL results are in bold. Note, $a_0 = -0.440$ and $a_1 = 0.300$ (see DTS).

The (substantially) weaker dissipation in the CASL integration is the result of being able to retain enstrophy to much finer scales. This is seen most directly in Fig. 4, which shows the enstrophy spectrum $\Omega(k, t)$ at the time of peak enstrophy dissipation $-\dot{Q}$ compared amongst all cases after rescaling as in DTS (with Reynolds number as defined below). At small k (large scales) the spectra converge, while at large k the CASL spectrum extends significantly further with an approximate k^{-1} scaling, consistent with Batchelor's (1969) theory of 2D turbulence [1] (but see DTS & Refs. for why Batchelor's theory is inconsistent).

Finally, we compare the evolution of enstrophy dissipation $-\dot{Q}$ among all integrations in Fig. 5 (left) and the Reynolds number rescaled evolution $-f(Re)\dot{Q}$ vs $t/f(Re)$ in Fig. 5 (right). Here, we have used $f(Re) = a_0 + a_1 \ln Re$ which, from a linear least-squares fit, best collapses the *pseudo-spectral* data (see DTS). For these data, the Reynolds number is defined by $Re \equiv \langle |\nabla \psi|^2 \rangle / \nu \omega_{\mathrm{rms}}$, which for the 8192^2 integration is 2.12×10^5. Applying the same scaling to the CASL data, specifically equating the peak enstrophy dissipation to $1/f(Re)$, we obtain an effective Reynolds number of approximately 3.80×10^7. A pseudo-spectral integration of comparable Reynolds number would require a grid of approximately $100\,000^2$, since the maximum Reynolds number typically scales with the square of the grid resolution.

Note, we are not claiming that the CASL integration generates a solution of the Navier–Stokes equations with finite viscosity. The main point is rather that the CASL integration produces the same enstrophy dissipation as the Navier–Stokes equations, but at a much higher Reynolds number than can be presently achieved with other methods.

We conclude with a comment on the cost of carrying out these integrations. The CASL integration required 5.34 h on a single 2.40 GHz Intel processor to reach 30 time units. The 8192^2 pseudo-spectral integration required approximately 8 days of computer power, using 256 2.00 GHz AMD Opteron processors, to reach 19 time units. It is not difficult to see that there is an enormous difference in cost – and the pseudo-spectral integration is much more diffusive! Taking into account the difference in Reynolds number and the difference in computational efficiency, we estimate that $\mathcal{O}(10^8)$ times more computer power would be required for a comparable pseudo-spectral integration.

The CASL algorithm is not just available to study idealised 2D flows. It has been extended in many ways, for instance in the simulation of 3D non-hydrostatic rotating stratified flows [4]. Work is underway to extend the algorithm to incorporate non-conservative effects such as forcing. Further details, including codes, are available at http://www.casl.org.uk.

References

[1] G.K. Batchelor, Computation of the energy spectrum in homogeneous two-dimensional turbulence, Phys. Fluids 12 (1969) 233–239.
[2] D.G. Dritschel, Contour surgery: a topological reconnection scheme for extended integrations using contour dynamics, J. Comput. Phys. 77 (1988) 240–266.
[3] D.G. Dritschel, M.H.P. Ambaum, A contour-advective semi-Lagrangian numerical algorithm for simulating fine-scale conservative dynamical fields, Quart. J. Roy. Meteorol. Soc. 123 (1997) 1097–1130.
[4] D.G. Dritschel, Á. Viúdez, A balanced approach to modelling rotating stably-stratified geophysical flows, J. Fluid Mech. 488 (2003) 123–150.
[5] D.G. Dritschel, C.V. Tran, R.K. Scott, Revisiting Batchelor's theory of two-dimensional turbulence, J. Fluid Mech. 591 (2007) 379–391.
[6] T.Y. Hou, R. Li, Dynamic depletion of vortex stretching and non-blowup of the 3-D incompressible Euler equations, J. Nonlinear Sci. 16 (2006) 639–664.